JOURNAL OF PROPULSION AND POWER
Vol. 23, No. 6, November–December 2007

Effect of Recess on the Spray Characteristics of Liquid–Liquid Swirl Coaxial Injectors

Dongjun Kim,* Poonggyoo Han,† Ji-Hyuk Im,‡ Youngbin Yoon,§ and Vladimir G. Bazarov¶
Seoul National University, Seoul 151-742, Republic of Korea

DOI: 10.2514/1.30450

The effects of recess in a liquid–liquid swirl coaxial injector on the spray characteristics have been investigated by measuring the spray angle and breakup length in eight cases of recess length. The orifice recess, a geometric parameter, has a strong influence on the spray and mixing characteristics by varying the interaction point between two liquid sheets. The variation of the recess length resulted in three different injection regimes: external, tip, and internal mixing injection. The coaxial spray characteristics in the external mixing injection regime are found to be mainly governed by the merging phenomenon and momentum balance between two liquid sheets. In the internal mixing injection regime, an impact wave is generated by the impingement of the inner spray on the outer liquid film inside the injector. The amplitude of the impact wave is gradually attenuated due to the fluid viscosity, flowing along the outer injector wall after impingement. This attenuation of the impact wave according to the recess length could affect the stability of a liquid sheet; therefore, the breakup length is found to increase with the increase in recess number.

Nomenclature

d_0	=	diameter of orifice exit
h_0	=	annular liquid sheet thickness at orifice exit
L_c	=	contact length, $(r_o - r_i)/\tan\theta_i$
L_r	=	recess length
$\dot{m}$	=	mass flow rate
P_{is}	=	interspace pressure between inner and outer sprays
RN	=	recess number
r	=	orifice radius
u	=	axial velocity
We	=	Weber number, $\rho u^2 h_0/\sigma$
w	=	tangential velocity
α	=	decay coefficient
ΔP	=	injection pressure difference
η_{ini}	=	initial wave amplitude near the impingement point
η_0	=	wave amplitude at the injector exit
θ	=	spray half-angle
μ	=	liquid viscosity
ρ	=	liquid density
σ	=	surface tension

Subscripts

i	=	inner injector or inner spray
o	=	outer injector or outer spray

I. Introduction

FAST atomization, uniform mass distribution, and mixing of propellants have great influence on combustion efficiency in liquid rocket engines. The injector is an essential device in the precombustion stage which involves atomization, evaporation, and mixing. Many types of injectors, such as a like- or unlike-doublet, triplet, pintle, and coaxial type have been used in liquid rocket engines. Extensive studies have been carried out to understand the effects of injection conditions and injector geometries on spray characteristics for several decades. Coaxial injectors, consisting of an inner injector surrounded by a concentric annular outer injector, are widely used in liquid rocket engines. Their advantages include high performance and stability with broad ranges of operation due to the efficient atomization and mixing of uniformly distributed propellants, as well as lower precision level requirements for manufacturing technology [1,2].

Coaxial injectors can be classified based on the combination of propellant phases used, such as gas–gas, gas–liquid, and liquid–liquid. Many investigations on the spray and breakup characteristics of coaxial injectors with a central liquid jet and annular gas jet have been performed [3,4]. The atomization of a shear coaxial injector is achieved through the transfer of kinetic energy from a high-speed gas stream to a liquid jet. Hadalupas and Whitelaw [3] observed the variation of mean drop size and spray width in response to changing the injection conditions and geometries, such as orifice diameters and recess lengths. They suggested that an optimal injector design could be established by simultaneously considering the drop size and spread of spray. Sankar et al. [4] reported that flow properties, such as surface tension and viscosity, had a crucial role in the atomization process.

When the phases of propellants were in a liquid–liquid combination, the swirl injectors were used as both the inner and outer injectors for efficient atomization and mixing. Liquid-–liquid swirl coaxial injectors have been widely used in liquid rocket engines to take advantage of their higher mixing efficiency within the short length of the combustion chamber [5–7]. Seol et al. [8] performed a visualization study on the interaction of the inner and outer liquid jets of a dual-orifice injector. They found that the spray interaction between two liquid jets was affected by the ambient pressure distribution around the jets. However, the study was restricted to low injection pressure where the conical liquid sheets did not fully diverge. Sivakumar and Raghunandan [6,7] carried out systematic experiments on the mutual interaction between thin coaxial liquid sheets. They concluded that the merging and separating process of two liquid sheets, which exhibited hysteresis, can lead to a significant

Received 14 February 2007; revision received 22 June 2007; accepted for publication 13 July 2007.

*Ph.D., School of Mechanical and Aerospace Engineering; currently at Rotem Co.; kan31@rotem.co.kr.
†Principal Research Engineer, Rotem Co.; pghan@hanmail.net.
‡Ph.D. Candidate, School of Mechanical and Aerospace Engineering; noname01@snu.ac.kr.
§Professor, Institute of Advanced Aerospace Technology, School of Mechanical and Aerospace Engineering, San 56-1, Shillim-dong, Gwanak-gu; ybyoon@snu.ac.kr.
¶Professor, Dynamic Processes Division of the Rocket Engines Chair, Moscow Aviation Institute; vgb2@mai.ru.

variation in the drop size. This variation can be related with engine throttling.

The geometric parameters of the injector, as well as the injection conditions, play a dominant role in the spray characteristics of a coaxial injector. In particular, the recess in a coaxial injector is configured so that the exit of the inner injector is located inwardly at a certain length from the exit of the outer injector. This recess has been widely used to increase both atomization and mixing efficiencies. Various investigations on the effect of a recess in gas–liquid coaxial injectors have been conducted [9–12]. Turbulent mixing, taking place within a larger recess, gives rise to improved atomization as well as increased evaporation of larger droplets. Kendrick et al. [12] reported that when recessed inside the hydrogen tube, the combustion products both block and add heat to the annular hydrogen flow, increasing the hydrogen velocity, and thus the momentum ratio of annular hydrogen to the center liquid oxygen (LOX) jet at the injector exit. These actions enhance jet breakup and lead to a small pressure loss within the injector. A recess also has a positive effect on the flame stabilization by inducing recirculation flows inside the recessed region which are insensitive to pressure disturbances in the main chamber [9,12].

In the case of a liquid–liquid swirl coaxial injector, Sivakumar and Raghunandan [5] measured the drop size variation while varying the recess length of an inner injector. Interestingly, they found that the recess had a negative effect on atomization because the internal interaction of two liquid sheets leads to the increase of effective sheet thickness. Kim et al. [13] examined the effects of liquid oxygen post recess on the combustion characteristics for unielement LOX/kerosene swirl coaxial injectors in four cases of recess length. They found that the combustion chamber pressure increased as the recess number increased at the same mass flow rate and O/F ratio.

The main objective of this study is to investigate the spray characteristics of a liquid–liquid swirl coaxial injector with various injection conditions and recess configurations. Ultimately, we would like to understand the phenomena of the interaction between two liquid sheets and the effects of different recess lengths by observing the spray shape, spray angle, and breakup length.

II. Experimental Methods

A. Swirl Coaxial Injector

The liquid–liquid swirl coaxial injector used in the experiments consisted of three parts: an inner injector, an outer injector, and an injector case, as shown in Fig. 1. The interior orifice diameters of the inner and outer injectors were 2 and 6 mm, respectively. The inner injector had three tangential entries with a diameter of 1 mm at every 120 deg and the outer injector had two tangential entries with a diameter of 0.85 mm at every 180 deg. The lip thickness of the inner injector was 1 mm, and thus, the gap size between the inner and the outer injectors was 1 mm.

The recess is a geometric variable of coaxial injectors. In some previous studies, the recess length has been normalized by the interior diameter of an inner injector or gap size between the inner and the outer injector. Burick [11] studied the mixing and atomization characteristics of several gas–liquid coaxial injectors with the variation of injector geometry as well as injector operating conditions and showed the resulting data according to the normalized oxidizer post recess defined as the ratio of recess length to the inner oxidizer orifice diameter. Sivakumar and Raghunandan [5] normalized the recess length of a liquid–liquid swirl coaxial injector by the gap size between the inner and the outer injector. However, this normalization can only be adopted for specific injector designs used in their respective studies. In a swirl coaxial injector, using liquid–liquid propellant with a recess, the interaction position of two liquid sheets has a significant influence on the resultant coaxial spray characteristics and the spray angle of an inner injector determines the interaction position in the recess region. Thus, in this study, a new dimensionless recess number RN, in a swirl coaxial injector, considering the spray angle of an inner injector, is defined as the ratio of the recess length L_r to the contact length L_c as shown in Fig. 2:

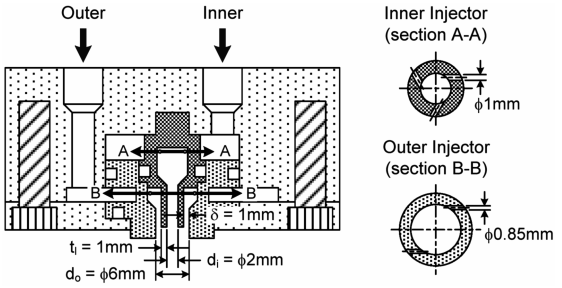

Fig. 1 Schematic of a swirl coaxial injector.

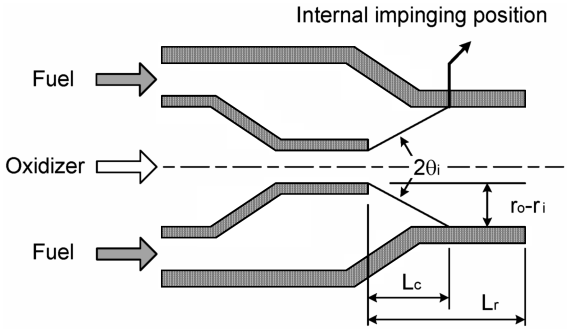

Fig. 2 Schematic of a coaxial injector with recess.

$$RN = \frac{L_r}{L_c}, \quad \text{where } L_c = \frac{r_o - r_i}{\tan\theta_i} \tag{1}$$

In this notation, the contact length L_c defines the length from an inner injector exit to the position where the liquid sheet injected from an inner swirl injector impinges the nozzle wall of an outer injector. r_o is the orifice radius of an outer injector and r_i is the orifice radius of an inner injector. The inner spray half-angle θ_i in Eq. (1) corresponds to the spray half-angle of the inner jet in the absence of an outer jet. Therefore, the recess number RN is a reference value that depends on the injector geometries and operating conditions. The recess lengths in Table 1 can be converted into dimensionless recess numbers according to a spray half-angle of inner sprays.

B. Experimental Conditions

In liquid–liquid swirl coaxial injectors, two different liquids are involved as fuel and oxidizer. However, in this study, to describe the spray behavior of two liquid sheets, the experiments were conducted using identical fluids of water as both inner and outer injectors. The coaxial liquid sheet characteristics are described in terms of Weber number defined as $We = \rho u^2 h/\sigma$, where ρ is the liquid density and σ the surface tension. A determination of the thickness of a liquid sheet was made by the empirical relation of Eq. (2) proposed by Suyari and Lefebvre [14]:

$$h_0 = 2.7\left[\frac{d_0 \dot{m}\mu}{\rho \Delta P}\right]^{0.25} \tag{2}$$

Here, d_0 is the diameter of the exit orifice, $\dot{m}$ the mass flow rate, μ the liquid viscosity, and ΔP the injection pressure drop. The axial velocity u was calculated by the equation of mass flow rate as follows:

$$u = \frac{\dot{m}}{\rho\pi(d_0 - h_0)h_0} \tag{3}$$

Table 1 shows the experimental conditions and parameters. First, for the study on the effect of injection conditions, Weber numbers were varied from 109 to 939 for an inner injector and from 47 to 385 for an outer injector. This corresponded to the injection pressure drop from 1 to 6 bars for both inner and outer injectors, and mass flow-rate

Table 1 Experimental conditions and parameters

	Inner injector	Outer injector
Effect of injection conditions		
Weber number, We	109, 261, 419, 578, 750, 939	47, 120, 187, 255, 335, 385
Recess length, mm	0 (without recess), 5 (with recess)	
Effect of recess configurations		
Weber number, We	109, 261, 419, 578, 750, 939	385 (fixed)
Recess length, mm	0, 2, 3, 4, 5, 6, 7, 8	

range of 7.97 to 23.48 g/s for an inner injector and 4.27 to 11.86 g/s for an outer injector. The experiments were conducted in two geometric cases, recess lengths of 0 (without recess) and 5 mm (with recess). Second, for the study on the effect of recess configurations, the experiments were performed for eight cases of recess length as shown in Table 1. The inner Weber number was varied from 109 to 939, while the outer Weber number was fixed at $We_o = 385$.

C. Experimental Techniques

The spray angle and breakup length were measured from the instantaneous spray images taken by indirect photography. Stroboscopic light with a luminous time of less than 4 μs was illuminated through translucent paper. The exposure time of a camera (Canon EOS 20D, 3504 × 2336) was set to be identical to the flash interval of the stroboscope to take one image per flash without extra synchronization. The spray angle was obtained from the angle between the injection axis and the connecting line of the orifice exit and the detected spray edge using an in-house code, as shown in Fig. 3. Although several possible criteria for the breakup length have been defined in the literature, the present study defines the breakup length as the continuous sheet length measured from the nozzle exit to the point where breakup occurs. To reduce the uncertainties of breakup length, the measurements were performed at the same radial location of the spray center. For the measurement of the spray angle and the breakup length, values acquired from 60 instantaneous images were averaged for each experimental case and deviations of data were less than 10% from their mean values as shown in Figs. 7a and 9.

A laser reflection method was used to measure the wave frequency on the liquid sheet surface as shown in Fig. 4. A He–Ne laser beam illuminated on the liquid sheet at 4 mm downstream from the injector exit. The wavy surface reflected the incident laser beam and a photodetector inclined to the incident beam detected the reflected beam according to the wavy motion. This signal of the reflected beam was recorded by a PULSE system (B&K Co. 3560C) and the wave frequency on the liquid sheet surface can be measured by a fast Fourier transform (FFT) analysis.

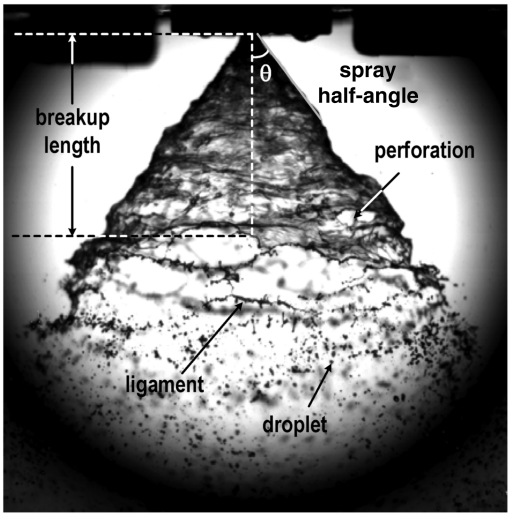

Fig. 3 Breakup pattern of a swirling liquid sheet and definitions of spray characteristics parameters.

III. Effect of Injection Conditions

A. Spray Shapes: External or Internal Mixing Injection

Typically, if the mixing and interaction of coaxial spray occurs inside the injector, namely, in the recess region, we call this an internal mixing injection; otherwise, we call this an external mixing injection. In Fig. 5, the coaxial spray shapes of both external and internal mixing injections are shown to be affected by increasing the Weber numbers of an inner (We_i) and an outer injector (We_o). In the external mixing injections of the coaxial injector without recess, a transition from separate to merged spray is observed. For $We_o = 47$, the coaxial sprays merge regardless of the increase of We_i, due to the onion shape of the outer spray. For $We_o = 120$ and 187, the coaxial sprays with $We_i = 109$ remain separate; however, a further increase of We_i leads to merging of the two liquid sheets. For $We_o \geq 255$, the coaxial sprays without recess always merge regardless of We_i, although the spray angle of an outer injector alone (Fig. 5d) is larger than that of an inner injector alone (Figs. 5e and 5j).

Figure 6 shows the schematic diagram of the merging process. It is known that the pressure difference between the liquid sheets causes contraction of the spray [15]. Once the spray is discharged, entrainment of ambient gas is generated at the inner and outer surfaces of the spray. However, the interior gas volume is limited by the spray so that a pressure difference between the inner and the outer gas is produced. In the external mixing injection of the coaxial injector without recess, the interior ambient gas volume of the outer swirling sheet is smaller than that of the outer spray alone due to the existence of inner spray. The decrease in the interspace pressure P_{is}, in the region between outer and inner liquid sheets, caused by the entrainment of ambient gas, makes the two liquid sheets approach each other. During the merging process, the interspace pressure gradually decreases from $(P_{is})_s$ at a separate stage to $(P_{is})_m$ at a merged stage. As the liquid sheet velocity increases, the interspace

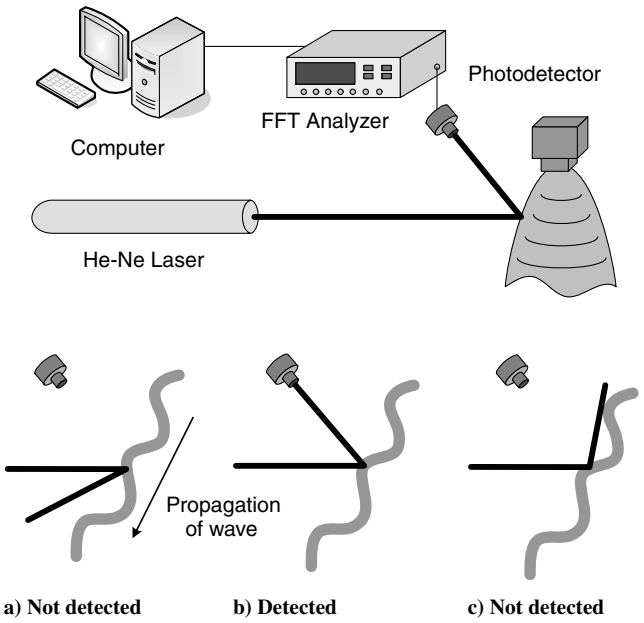

Fig. 4 Schematic diagram of the reflective laser technique for measurement of the wave frequency on the liquid sheet surface.

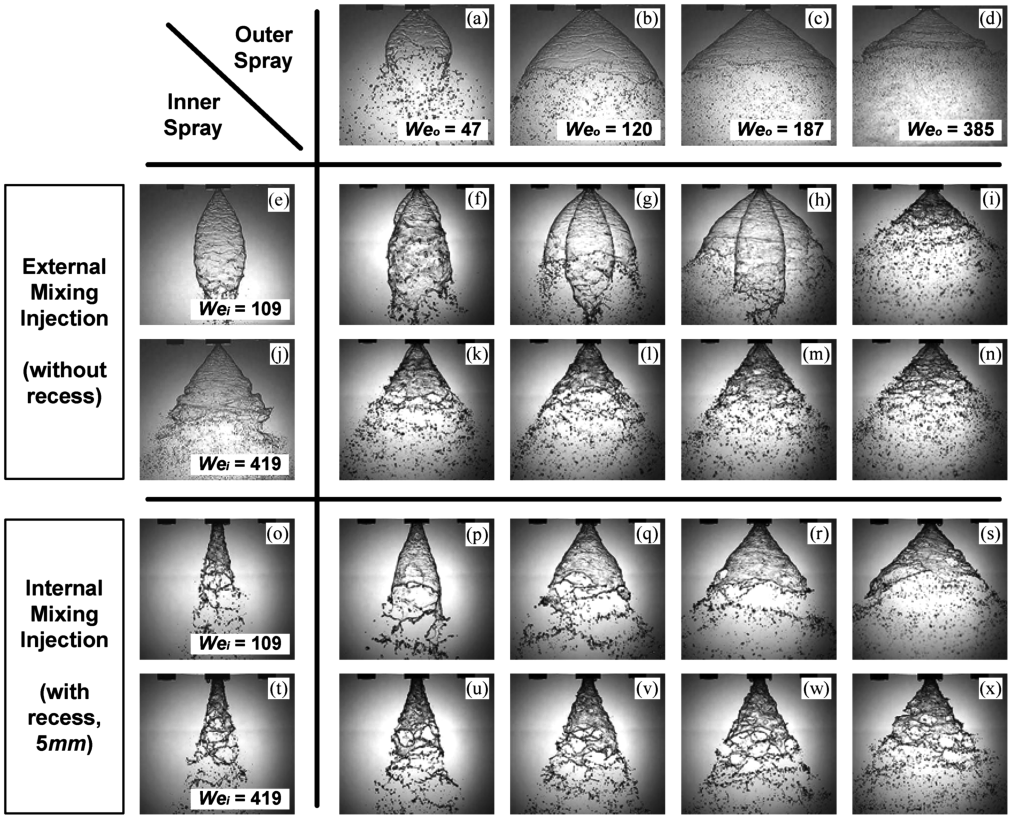

Fig. 5 Coaxial spray shapes according to the Weber numbers of an inner and an outer injector.

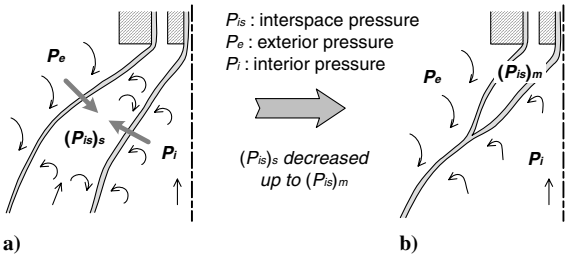

Fig. 6 Schematic diagram of the merging process from a) separate stage to b) merged stage due to the decrease in interspace pressure between two liquid sheets.

pressure between two liquid sheets decreases more by the swirl effect. Thus, separate coaxial spray was not observed at higher We_i or We_o. For the overall coaxial spray in an external mixing injection, the breakup length decreases and the spray angle increases with increasing We_i.

In the internal mixing injection of the coaxial injector with recess, separate discharging phenomena are not found even at the very low We_i, because the inner and outer sprays coalesce and mix on the outer injector wall. Compared to the coaxial sprays in external mixing injection, the coaxial spray of the internal mixing injection shows a relatively uniform shape with a narrower spray angle and slightly longer breakup length under the same injection conditions. When the inner Weber number We_i is increased, a decrease of the coaxial spray angle is observed as shown in Fig. 5. On the other hand, the breakup length of the coaxial spray decreases due to the increase in injection velocity. The detailed results concerning the spray angle and breakup length are described in the next section.

B. Spray Angle

The spray angle, which characterizes the spatial distribution of droplets, has a strong influence on ignition performance, the interactive characteristics of a multi-element injector, and on the cooling of the injector plate in rocket engines. Figure 7a shows the measurements of individual spray angles of the inner and outer injectors. In the case without recess, the inner spray shape undergoes a tulip stage and grows to a fully developed cone of approximately 77 deg after $We_i = 400$. However, the fully developed angle of a recessed inner injector is measured to be approximately 32 deg. In general, the tangent of a spray half-angle can be determined by the ratio of azimuthal velocity w to axial velocity u at the orifice exit. The interior diameter of the outer injector is 3 times larger than that of the inner injector so that the azimuthal velocity of the recessed inner spray at the final exit plane is about 3 times lower due to the conservation of angular momentum ($wr = \text{const}$). The outer spray also undergoes a tulip stage and grows to a fully developed cone of approximately 110 deg after $We_o = 200$.

To identify the spray angle change of an inner and outer liquid sheet in the external mixing injection according to the merging phenomenon, the coaxial spray angle was measured with varying We_o at a fixed $We_i = 109$, as shown in Fig. 7b. Two liquid sheets merge at $We_o = 47$, and thereafter, the inner and outer sheets are separately injected. After $We_o = 255$, the two liquid sheets merge again. These separate and merged shapes may be observed in Figs. 5f–5i. During the separate injection, the outer spray angle is smaller and the inner spray angle is larger than each individual spray angle. This results from the decrease in interspace pressure in the region between two liquid sheets, P_{is}. On the other hand, the merged spray angles are determined to be the values between the individual inner and outer spray angles for the same injection conditions. However, it is noted that the merged spray angle at $We_o = 47$ is close to the individual inner spray angle of approximately 61 deg, whereas the merged spray angles after $We_o = 255$ are close to the individual outer spray angles of approximately 108 deg. Therefore, it is expected that the merged coaxial spray angle is greatly influenced by the relative momentum change in either the inner or the outer liquid sheet.

The measured spray angles for different injection conditions are shown in Fig. 8. Figure 8a shows the coaxial spray angle with respect to the change in We_o and each symbol indicates the same We_i. For both cases of with and without recess, it is found that the coaxial

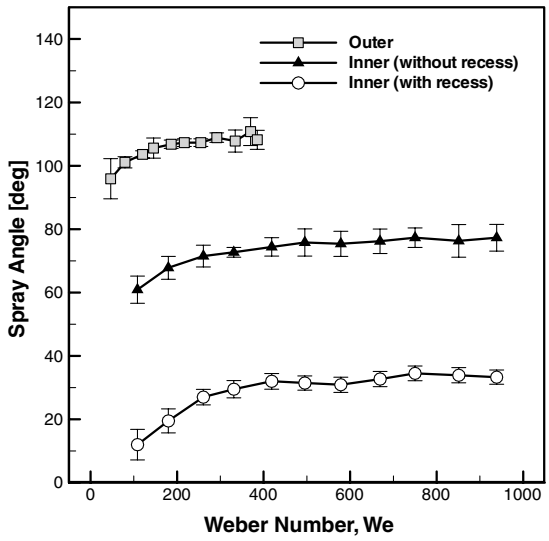

a)

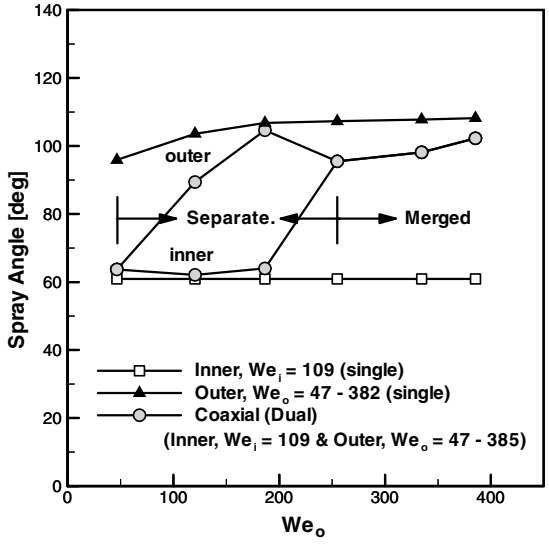

b)

Fig. 7 Spray angle variations: a) each individual injector according to the Weber number b) change from separated to merged spray according to the We_o.

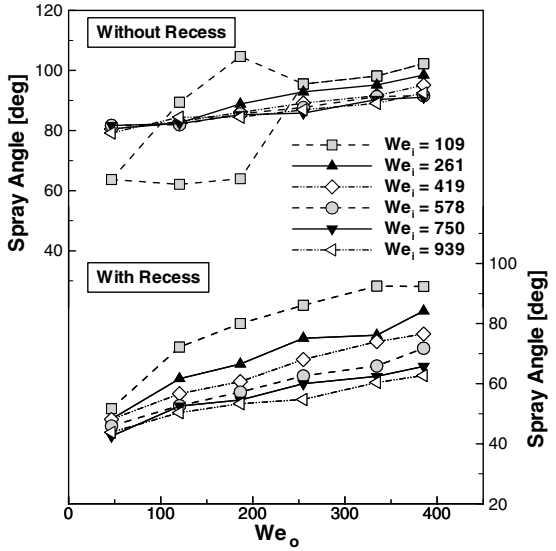

a)

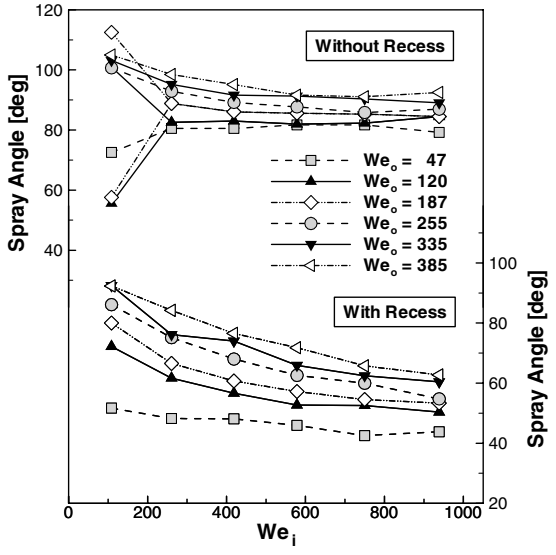

b)

Fig. 8 Spray angle variations: a) increasing the Weber number of an outer injector We_o; b) increasing the Weber number of an inner injector, We_i.

spray angle increases with the We_o. This may be due to an increase in the momentum of the outer liquid sheet of a relatively larger spray angle. Figure 8b shows the coaxial spray angle with respect to the change in We_i and each symbol indicates the same We_o. According to the increase of We_i, the coaxial spray angles in the external mixing injection are nearly invariant, while those in the internal mixing injection gradually decrease. Consequently, when the mass flow rate or momentum of the inner spray of a smaller spray angle is increased, the coaxial spray angle approaches the values of the individual inner spray angle and vice versa. Also, the coaxial spray angles of the cases without recess are larger than those of the cases with recess under the same injection conditions.

The merging of two liquid sheets is an inelastic process, in which the kinetic energy is dissipated as mechanical mixing energy and thus, momentum balance between two liquid sheets can be the determining factor for a coaxial spray angle after merging. Equations (4) and (5) are the conserved momentum equations in the axial and azimuthal directions by assuming steady and inviscid liquid and neglecting body forces:

$$\dot{m}_i u_i + \dot{m}_o u_o = (\dot{m}_i + \dot{m}_o) u \tag{4}$$

$$\dot{m}_i w_i + \dot{m}_o w_o = (\dot{m}_i + \dot{m}_o) w \tag{5}$$

Here, $\dot{m}$ is the mass flow rate, u is the axial velocity, w is the azimuthal velocity, and subscripts i and o represent an inner and an outer injector, respectively. The tangent of the spray half-angle can be predicted using the ratio of azimuthal velocity w to axial velocity u at the orifice exit so that the coaxial spray half-angle θ is obtained by dividing Eq. (5) by Eq. (4), as shown in Eq. (6).

$$\tan\theta = \frac{w}{u} = \frac{\dot{m}_i u_i \tan\theta_i + \dot{m}_o u_o \tan\theta_o}{\dot{m}_i u_i + \dot{m}_o u_o} \tag{6}$$

where

$$\tan\theta_i = \frac{w_i}{u_i}, \quad \text{and} \quad \tan\theta_o = \frac{w_o}{u_o}$$

Figure 9 shows the comparison between the measured and calculated coaxial spray angles using Eq. (6). Though the calculated coaxial spray angles agree well with the measured angles in the external mixing injection of the case without recess, the calculated values are a little larger than the measured angles in the internal

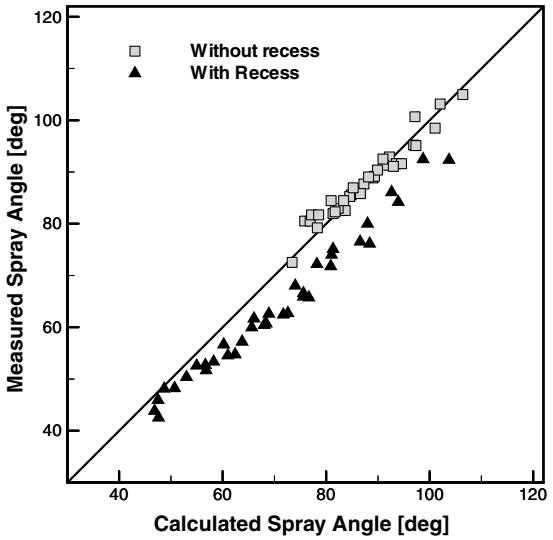

Fig. 9 A comparison between the measured and calculated spray angles.

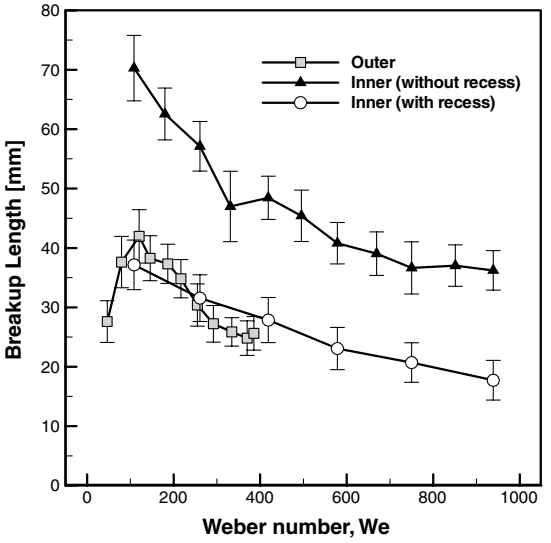

Fig. 10 Breakup length of each single injector according to the Weber number.

mixing injection of the case with recess. In the internal mixing injection, the merged liquid sheet flows along the interior wall of an outer injector after impingement. During this process, momentum loss results from the impact force by strong impingement of two liquid sheets and the friction force between liquid and the injector wall. Therefore, the measured coaxial spray angles in the cases with recess are smaller than the calculated angles. From these results, it may be expected that the coaxial sprays in the cases without recess are mainly under the control of the momentum balance between the two liquid sheets. However, the coaxial sprays of the cases with recess are influenced by the impingement as well as momentum balance between two liquid sheets.

C. Breakup Length

The measured individual breakup length of an inner and outer spray, with respect to the variation of Weber number is shown in Fig. 10. It is observed that the breakup length of an outer injector initially increased, reaches a maximum, and thereafter decreases in the correspondence with increasing We. The initial increasing trend could be explained by the onion shape before a fully developed cone as shown in Fig. 5. At low We, because the surface tension force acts dominantly on the conical liquid sheet of the outer injector against the inertia and centrifugal forces, the conical liquid sheet is not able to diverge radially. Thus, the liquid sheet breaks up near the injector exit as a result of a thick film thickness at low We. At $We = 120$ and higher, the breakup length of the outer spray decreases as a consequence of the sheet perforation by thinning of the liquid sheet thickness and of the aerodynamic wave caused by the ambient gas.

On the other hand, the breakup length of the inner spray gradually decreases with an increase in We, regardless of the existence of recess. The breakup length of a recessed inner injector is found to be shorter than that of a nonrecessed inner injector, as a consequence of the impingement of the inner spray on the interior wall of the outer injector. Also, a steep increase of breakup length in the case without recess at low We, which results from the developing process of a swirl injector, is not observed in the case with recess.

Figure 11 shows the measured breakup lengths of coaxial spray for different injection conditions together with the breakup lengths for the individual spray of an inner and an outer injector. The breakup lengths with varying We_o at each fixed We_i are shown in Fig. 11a. In the case without recess, the breakup lengths of coaxial spray are all short compared to those of the individual inner and outer sprays alone. At low We_i [=261 (▲) –419 (◇)], the variation of breakup length for coaxial spray is similar to that of the outer spray. However, if $We_i > 578$ (○), the coaxial spray breakup lengths are almost constant regardless of the increase in We_o. In the case with recess,

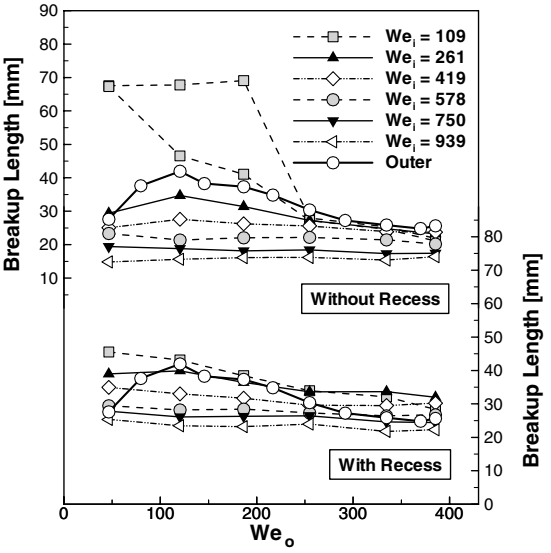

a)

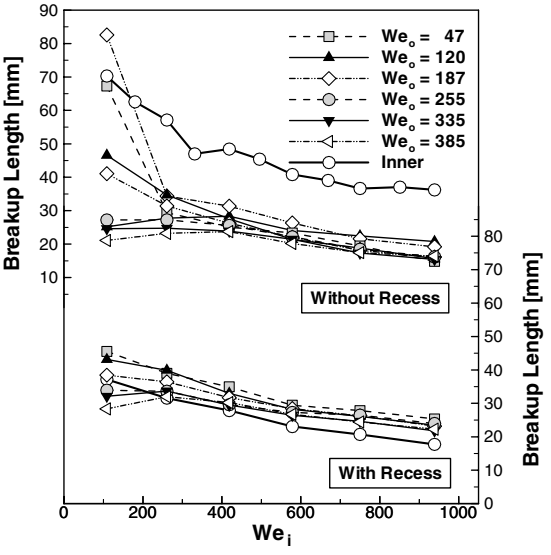

b)

Fig. 11 Breakup length variations: a) increasing the Weber number of an outer injector, We_o; b) increasing the Weber number of an inner injector, We_i.

when increasing the We_o, the breakup lengths slowly decrease at low We_i, but are almost constant at high We_i. Figure 11b shows the breakup lengths of coaxial sprays with respect to an increase in We_i. An obvious decay of breakup length with increase in We_i is observed in contrast with the variation resulting from a change in We_o. In both cases of external mixing injection regions without recess and internal ones with recess, the variation of coaxial spray breakup length is likewise similar to that of the inner spray at low We_o (=120–187); however, if $We_o > 255$, the breakup length until $We_i = 419$ ($\diamond$) is nearly invariant regardless of the increase in We_i. Consequently, it is found that the coaxial spray breaks up faster as We_i or We_o increases in both cases with and without recess.

IV. Effect of Recess Length

In the preceding section, the effects of injection conditions on the coaxial spray characteristics were investigated. The coaxial spray characteristics are found to be strongly influenced by the mixing position (external or internal mixing) of two liquid sheets depending on the existence of a recess configuration. In this section, the investigation is focused on the effect of recess length on the spray characteristics of a liquid–liquid swirl coaxial injector by reducing the orifice length of an inner injector. The outer Weber number We_o was fixed at 385 and the inner Weber number We_i was varied from 109 to 939 in order to change the impact force by an inner spray.

A. Spray Shapes

Figure 12 shows spray shapes of liquid–liquid swirl coaxial injectors with different recess numbers at a representative case of $We_i = 939$ and $We_o = 385$. The variation of the recess length results in three different injection regimes: external, tip, and internal mixing injection. The inner spray angle varies by changing We_i and thus, different recess numbers are calculated according to We_i even at the same recess length. Figures 13a–13c show the schematic diagrams illustrating the injection regimes. The diagrams were constructed from the edge detection of captured spray images.

1. *External Mixing Injection* ($0 \le RN < 1.0$)

The coaxial sprays in $0 \le RN < 1.0$ are defined as an internal mixing injection, where the interaction of two liquid sheets is not affected by the outer injector wall. The radial spray width in the external mixing injection is wider than that in the internal mixing injection. An inner and an outer liquid sheet of $RN = 0$ in Fig. 12a are

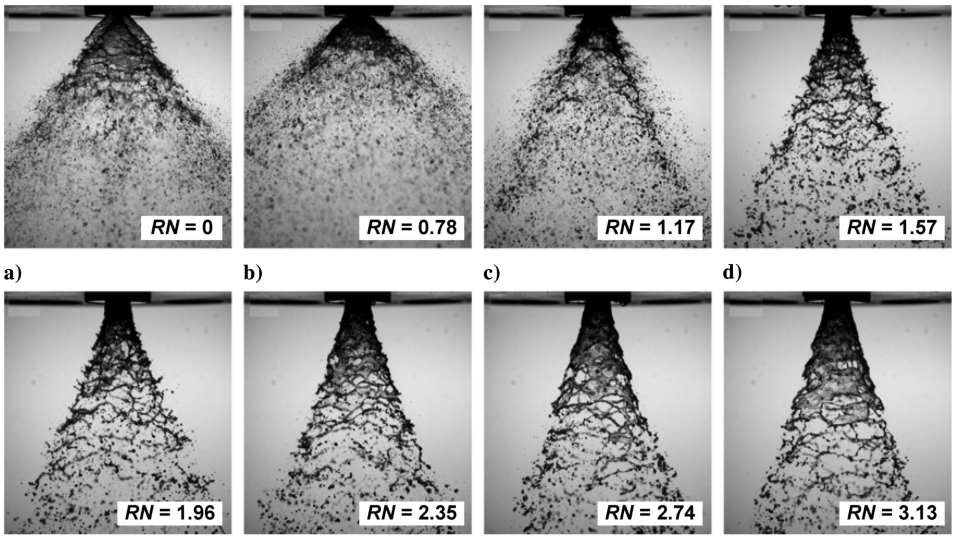

Fig. 12 Spray patterns according to the recess number at $We_i = 939$ and $We_o = 385$: a), b) are the external mixing injections ($0 \le RN < 1.0$); c) is the tip mixing injection ($1.0 \le RN \le 1.2$); and d)–h) are the internal mixing injections ($RN > 1.2$).

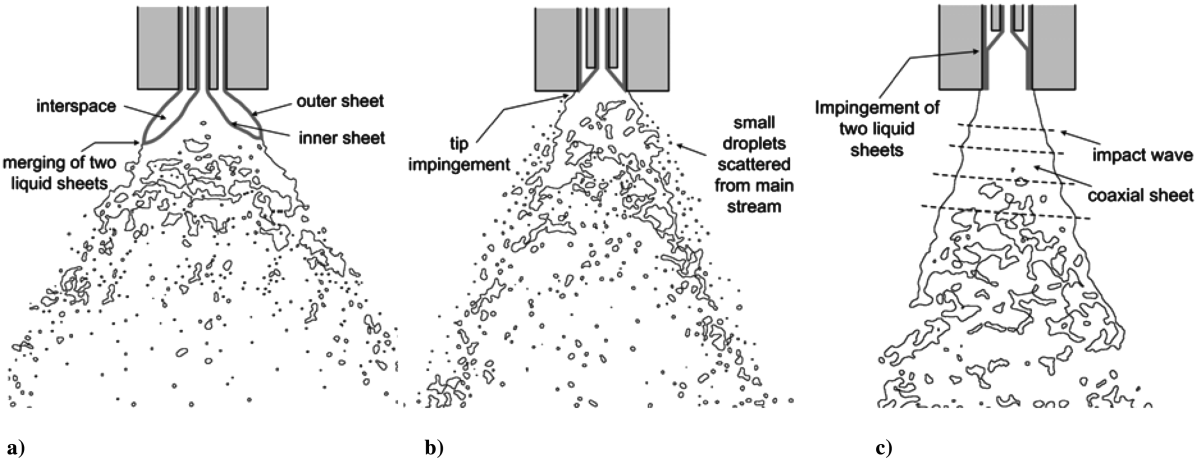

Fig. 13 Schematic diagrams illustrating the injection regimes with the change of recess length in the case of a liquid–liquid swirl coaxial injector extracting the edge from the spray images: a) external mixing injection, b) tip mixing injection, and c) internal mixing injection.

combined by the merging process explained in Fig. 6, and the merging point is separate from the injector exit plane (Fig. 13a). In the case of $RN = 0.78$, however, an apparent merging point is not observed as shown in Fig. 12b. Because an outer jet flows out, forming a thin liquid film, it may be seen that two liquid sheets meet directly under the outer injector exit plane. Thus, the spray shape is somewhat different from the case of $RN = 0$, such as a wider spray width and shorter breakup length.

2. Tip Mixing Injection ($1.0 \leq RN \leq 1.2$)

According to Eq. (1), the outer surface of an inner spray exactly meets at the outer injector exit tip when L_r is identical to L_c—that is, the recess number is unity. However, because the inner spray is discharged with its own thickness of about 380 μm, for example, at $We_i = 939$, two liquid sheets truly meet within the outer injector exit tip at a somewhat larger recess number than unity. From the simple geometric calculation with a film thickness of 380 μm and spray half-angle of 38.66 deg, the inner surface of the inner spray exactly meets at the outer injector exit tip when the recess number is about 1.2. Therefore, coaxial sprays at recess numbers from 1.0 to 1.2 are defined as tip mixing injection, where all interaction between two liquid sheets does not occur on the outer injector wall and a part of the inner spray impinges on the outer spray outside the injector. As shown in Fig. 12c, the liquid sheet is not observed, but fully atomized droplets with a narrow spatial distribution are observed, which is accompanied by tip impingement of an inner liquid sheet. Also, the small droplets are scattered outside the main stream of a spray as shown in Fig. 13b.

3. Internal Mixing Injection ($RN > 1.2$)

The spray shapes of $RN > 1.2$ are defined as internal mixing injection, where the interaction of two liquid sheets occurs inside the injector. Figures 12d–12h correspond to the internal mixing injection regime. The spray width decreases considerably due to the decrease of azimuthal velocity by impingement on the outer injector wall. When a recess length is shallow in the internal mixing injection (Fig. 12d), the liquid sheet surface is highly disturbed and the breakup length is found to be short. As the recess number increases, the coaxial liquid sheet becomes more stable and the liquid sheet breakup length becomes longer. This may be explained by the formation and decay of an impact wave by the internal impinging phenomenon of two liquid sheets inside the recess region; when the inner liquid sheet impinges on the outer liquid film flowing along the injector wall, the impact wave is formed. The amplitude of the impact wave gradually decays as the impinged sheet flows along the outer injector wall. A detailed description on the internal impinging phenomenon and its effects on the spray characteristics in the internal mixing injection region are discussed in the next section. Sivakumar and Raghunandan [5] reported that the larger-diameter droplets were produced, when the merging and mixing of two liquid sheets occurred inside the recess region. From Fig. 12, the larger droplets were likewise observed in the internal mixing injection due to the increase in the effective thickness of the liquid sheet.

B. Internal Impinging Phenomenon ($RN > 1.2$)

Previous studies of impinging jet injectors have indicated that an impact wave may dominate the atomization of high-speed turbulent impinging jets [16–18]. Dombrowski and Hooper [16] identified two different operating regimes of impinging jets: a laminar sheet regime, where the jets are laminar and jet velocities are less than about 5 m/s; and the impact wave dominated regime, where the jets can be either laminar or turbulent and the impact wave is generated from the jet impingement point. Although the breakup in a laminar sheet regime was reasonably predicted by linear theory, the comparisons between experimental results and linear stability-base predictions in an impact wave dominated regime indicated disagreements with respect to wavelength and breakup length [17]. Therefore, a fundamental study on the generation and growth or decay of an impact wave and its association with the subsequent atomization process is worthy of notice.

Figure 14 shows the schematics of internal impinging phenomenon occurring in swirl coaxial injectors with shallow and deep recess lengths. Because the injection conditions of two liquid sheets were fixed for both recess lengths, the initial amplitudes of the impact waves near the impingement point may be identical regardless of the recess length. However, in the presence of viscosity, the wave amplitude decays exponentially with the distance traveled according to $\eta = \eta_{\text{ini}} e^{-\alpha x}$, where η_{ini} is the initial wave amplitude near the impingement point ($x = 0$) and α is the decay coefficient [19]. The wave amplitude at the injector exit of a deep recess length $(\eta_0)_{\text{deep}}$ is smaller than that of a shallow recess length $(\eta_0)_{\text{shallow}}$ as shown in Fig. 14. The coaxial liquid sheet of a shallow recess length is more disturbed, and thus, the breakup length is shorter, which is supported by the spray shapes in Fig. 12. Therefore, the formation and decay of the impact wave by the internal impingement phenomena may have a strong influence on the spray characteristics in the internal mixing injection.

To identify the generation of impact waves by the impingement of two liquid sheets, the surface wave frequencies were measured for individual inner and outer sprays and also a mixed spray using a laser reflection method. It is well known that the disintegration of liquid sheets is caused by the growth of unstable waves at the interface due to the aerodynamic interaction between the liquid and ambient gas. There exists a dominant or most unstable wave corresponding to the highest growth rate of a wave amplitude. The measured wave frequencies in an inner and an outer sheet are about 2.3 kHz at $We_i = 939$ and 850 Hz at $We_o = 385$. This is the aerodynamic wave formed by interaction with the ambient gas. However, all of the recess lengths in the internal mixing injection give a peak amplitude at the frequency of about 180 Hz at the same injection condition ($We_i = 939$ and $We_o = 385$). This difference in frequency range can verify the presence of an impact wave formed by the impact of the two liquid sheets. Kim et al. [13] also observed the low frequency pressure fluctuations of about 200 Hz in the internal mixing injection by the combustion tests of a liquid–liquid swirl coaxial injector. However, for the external mixing injection, the pressure fluctuation level was relatively low and maintained steady-state values except initial and shutdown transient.

The surface fluctuation of the liquid sheet was obtained through 60 magnified images at the axial position of 4 mm from the injector exit for various recess lengths as shown in Fig. 15. The standard deviation of this surface fluctuation is shown in Fig. 16 and is found to decrease with an increase of recess length. Although the standard deviation does not directly indicate the wave amplitude, this deviation is related to the sheet fluctuation by the wave amplitude. These measurements can confirm the schematic diagrams of internal impingement phenomena as shown in Fig. 14.

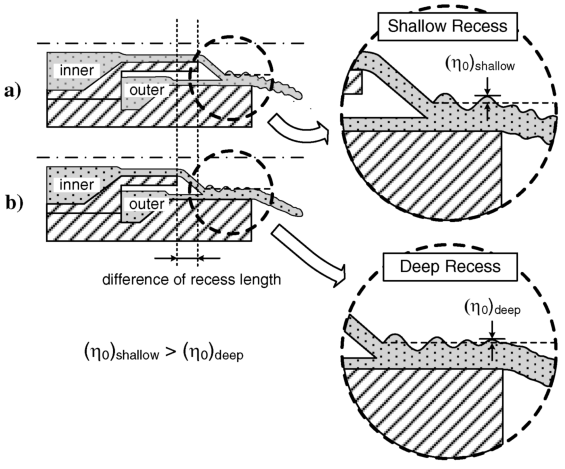

Fig. 14 Influences of internal interaction according to the recess lengths: a) shallow recess and b) deep recess.

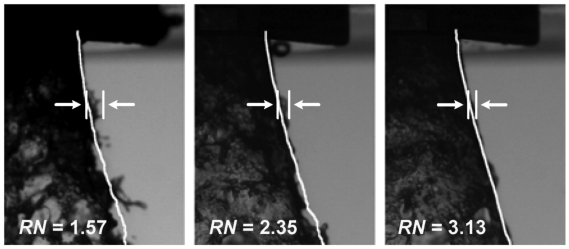

Fig. 15 Surface fluctuation of coaxial liquid sheet in the internal mixing injection by magnified images of $We_i = 939$ and $We_o = 385$ at $Z = 4$ mm. a) $RN = 1.57$; b) $RN = 2.35$; (c) $RN = 3.13$.

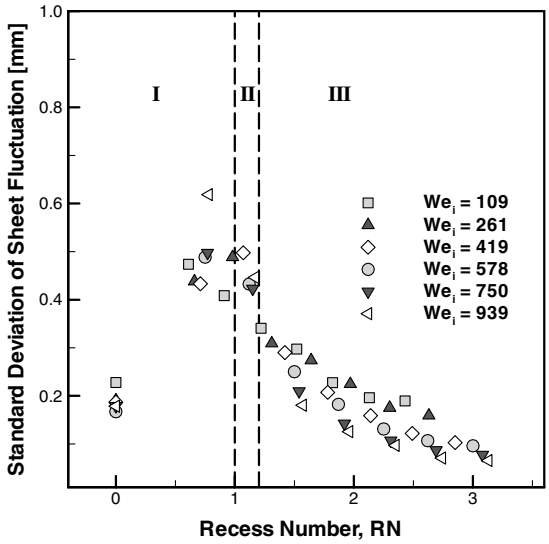

Fig. 16 Standard deviation of sheet fluctuations according to the recess number and We_i. I: external mixing injection, II: tip mixing injection, and III: internal mixing injection.

C. Spray Angle and Breakup Length

The variation of a coaxial spray angle with recess number and inner Weber number is shown in Fig. 17. The outer Weber number was fixed at $We_o = 385$. As explained in the preceding results of Fig. 9, the coaxial spray angle in the internal mixing injection is smaller than that in the external mixing injection due to the internal impingement of two liquid sheets on the outer injector wall. The maximum coaxial spray angle is observed at $0.6 < RN < 0.8$ except for $We_i = 109$ of an onion-shaped spray. The small variation of recess length in the external mixing injection has also a distinct influence on the resultant coaxial spray angle. For the case of $0.6 < RN < 0.8$, the interspace between the inner and outer sheet including the region inside the injector is small, and thus, the decrease in pressure in this region for $0.6 < RN < 0.8$ is relatively small as compared with $RN = 0$. Therefore, the coaxial spray angle of $0.6 < RN < 0.8$ is a little larger than that of $RN = 0$.

The coaxial spray angle at $1.0 < RN < 1.2$ in tip mixing injection is significantly reduced. All of the injection conditions in the tip mixing injection show a similar spray angle at the value of about 60 deg. In the internal mixing injection region, the spray angle is not affected by the recess number and is smaller than that in the tip mixing injection, at moderate We_i (≥ 419). As a whole, a smaller coaxial spray angle is observed at higher We_i. This is due to an increase in the momentum of an inner jet of a relatively small spray angle.

Figure 18 shows the variation of breakup length according to the recess number and inner Weber number at a fixed $We_o = 385$. Similar to the results of the spray angle in Fig. 17, the variation of the breakup length is different depending on whether the coaxial spray is in external, tip, or internal mixing injection. The closer the

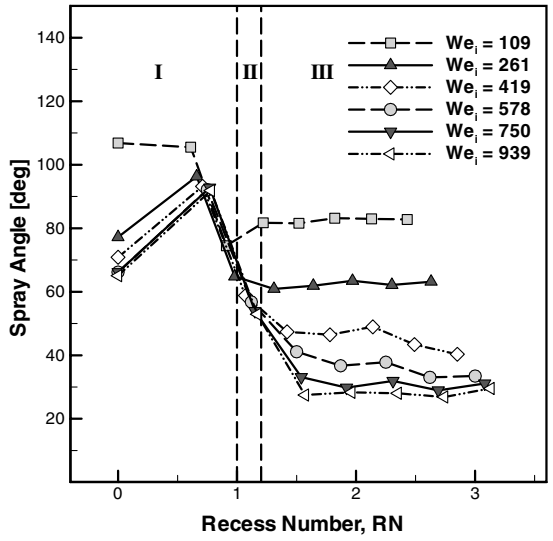

Fig. 17 Spray angle variation according to the recess number. I: external mixing injection, II: tip mixing injection, and III: internal mixing injection.

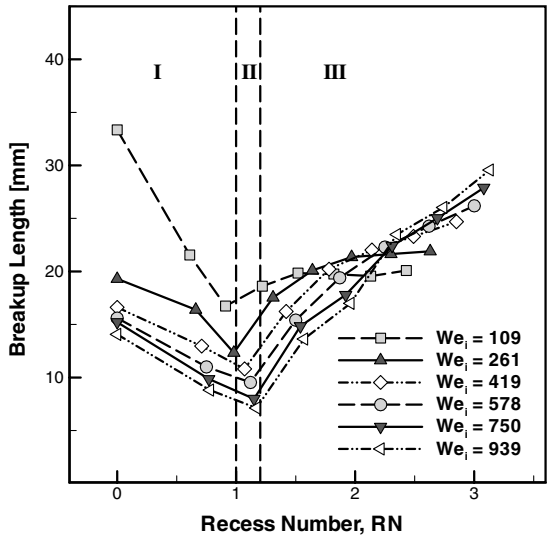

Fig. 18 Breakup length variation according to the recess number. I: external mixing injection, II: tip mixing injection, and III: internal mixing injection.

impingement point is from the injector exit, the shorter the breakup length of the coaxial spray. The minimum breakup length is observed in the tip mixing injection at $1.0 < RN < 1.2$. When increasing the recess number, the breakup length of the coaxial spray decreases in the external mixing injection region. On the contrary, the breakup length increases in the internal mixing injection region except for $We_i = 109$. As discussed previously, the trend of increasing breakup length in the internal mixing injection region is due to the amplitude decay of an impact wave caused by the internal impinging phenomenon. The variation of breakup length at $We_i = 109$ in the internal mixing injection is somewhat different compared with the other injection conditions. A weak impact force may result in the almost constant breakup length at $We_i = 109$.

Clark and Dombrowski [20] suggested that the breakup length of a liquid sheet is affected by the amplitude of the wave at the injector exit η_0. Because they dealt with a single conical liquid sheet, the disturbances observed on the liquid sheets were naturally caused by wave motions within the air core upstream of the injector. However, the amplitude of the impact wave by impingement of two liquid sheets was higher than that by natural wave motions. Hence, it could be assumed that the wave by impingement of two liquid sheets

dominantly controls the breakup process of a coaxial spray. The impingement of an inner jet with sufficient momentum results in the formation of an impact wave on the coaxial liquid sheet, and the decay of wave amplitude according to recess length has significant influences on the breakup length.

V. Conclusions

The effects of an orifice recess length on the spray characteristics of a liquid–liquid swirl coaxial injector were investigated by observing the spray shape, spray angle, and breakup length of the resultant coaxial spray. The orifice recess in a coaxial injector is a geometric parameter, which is used to control the spray and mixing characteristics by varying the interaction point between two liquid sheets. First, experiments were conducted using a coaxial injector with different combinations of inner and outer flow conditions, with and without orifice recesses, and the spray angle and breakup length were measured for individual inner and outer sprays, as well as the mixed spray. The investigation revealed that the coaxial spray characteristics were strongly influenced by the mixing position of two liquid sheets: external or internal mixing injection. The characteristics of coaxial sprays generated without recess in the external mixing injection region were mainly under the control of the momentum balance between the two liquid sheets. However, the characteristics of coaxial sprays generated with recess, in the internal mixing injection region, were influenced by impingement as well as momentum balance between the two liquid sheets.

Secondly, a detailed study on the effect of recess length on the spray characteristics of a liquid–liquid swirl coaxial injector was performed by varying the inner flow rate at a fixed outer flow rate in order to examine the internal impingement phenomena. When the inner liquid sheet impinged on the liquid film on the outer injector wall, an impact wave was formed. The presence of an impact wave was verified by the difference in frequency measurements of liquid sheet surfaces for individual inner and outer sprays and also the mixed spray in the internal mixing injection. The measured frequency of an impact wave was relatively low as compared with the aerodynamic waves of individual inner and outer sprays. However, in the presence of viscosity, the wave amplitude decays exponentially with the distance traveled along the outer injector wall. Accordingly, the wave amplitude at the injector exit of a deep recess length is smaller than that of a shallow recess length, and the coaxial liquid sheet of a shallow recess length is more disturbed, and thus, the breakup length is shorter. Therefore, the formation and decay of the impact wave by the internal impingement phenomena may have a strong influence on the spray characteristics in the internal mixing injection. In the internal mixing injection, the internal impingement of propellants inside the injector can enhance the mixing characteristics, while the impact wave by the impingement can affect the stability of propellants in the feedline. Therefore, the selection of suitable recess length is recommended by considering both performance and stability.

Acknowledgments

This research was supported by the Korea Science and Engineering Foundation (KOSEF) grant funded by the Ministry of Science and Technology (MOST) of the Korean government (R01-2007-000-11071-0) and Institute of Advanced Aerospace Technology.

References

[1] Lefebvre, A. H., *Atomziation and Sprays*, Hemisphere, Washington, D.C., 1989.

[2] Bayvel, L., and Orzechowski, Z., *Liquid Atomization*, Taylor and Francis, Wasington, D.C., 1993.

[3] Hadalupas, Y., and Whitelaw, J. H., "Characteristics of Sprays Produced by Coaxial Airblast Atomizers," *Journal of Propulsion and Power*, Vol. 10, No. 4, 1994, pp. 453–460.

[4] Sankar, S. V., Brena de la Rosa, A., Isakovic, A., and Bachalo, W. D., "Liquid Atomization by Coaxial Rocket Injectors," *29th Aerospace Sciences Meeting*, AIAA, Reston, VA, 7–10 Jan. 1991.

[5] Sivakumar, D., and Raghunandan, B. N., "Role of Geometric Parameters on the Drop Size Characteristics of Liquid-Liquid Coaxial Swirl Atomizer," *Atomization and Sprays*, Vol. 8, No. 5, 1998, pp. 547–563.

[6] Sivakumar, D., and Raghunandan, B. N., "Hysteretic Interaction of Conical Liquid Sheets from Coaxial Atomizers: Influence on the Spray Characteristics," *Physics of Fluids*, Vol. 10, No. 6, 1998, pp. 1384–1397. doi:10.1063/1.869663

[7] Sivakumar, D., and Raghunandan, B. N., "Formation and Separation of Merged Liquid Sheets Developed from the Mixing of Coaxial Swirling Liquid Sheets," *Physics of Fluids*, Vol. 15, No. 11, 2003, pp. 3443–3451. doi:10.1063/1.1616032

[8] Seol, W. S., Han, Y. M., Yoon, M. S., Lee, D. S. and Yagodkin, V. I., "A Visualization Study of Dual Spray Interaction of a Dual-Orifice Fuel Injector at Low Pressure Drop," *Journal of Flow Visualization and Image Processing*, Vol. 5, No. 1, 1998, pp. 41–50.

[9] Mayer, W., and Tamura, H., "Propellant Injection in a Liquid Oxygen/Gaseous Hydrogen Rocket Engine," *Journal of Propulsion and Power*, Vol. 12, No. 6, 1996, pp. 1137–1147.

[10] Mayer, W., Schik, A., Talley, D., and Woodward, R., "Atomization and Breakup of Cryogenic Propellants Under High-Pressure Subcritical and Supercritical Conditions," *Journal of Propulsion and Power*, Vol. 14, No. 5, 1998, pp. 835–842.

[11] Burick, R. J., "Atomization and Mixing Characteristics of Gas-Liquid Coaxial Injector Elements," *Journal of Spacecraft and Rockets*, Vol. 9, No. 5, 1972, pp. 326–331.

[12] Kendrick, D., Herding, G., Socuflaire, P., Rolon, C., and Candel, S., "Effects of a Recess on Cryogenic Flame Stabilization," *Combustion and Flame*, Vol. 118, No. 3, 1999, pp. 327–339. doi:10.1016/S0010-2180(98)00168-0

[13] Kim, S.-H., Han, Y.-M., Seo, S., Moon, I.-Y., Kim, J.-K., and Seol, W.-S., "Effects of LOX Post Recess on the Combustion Characteristics for Bi-Swirl Coaxial Injector," *The 41st AIAA/ASME/SAE/ASEE Joint Propulsion Conference and Exhibit*, AIAA, Reston, VA, 10–13 July 2005.

[14] Suyari, M., and Lefebvre, A. H., "Film Thickness Measurements in a Simplex Swirl Atomizer," *Journal of Propulsion and Power*, Vol. 2, No. 6, 1986, pp. 528–533.

[15] De Corso, S. M., and Kenemy, G. A., "Effect of Ambient Fuel Pressure on Nozzle Spray Angle," *ASME Transactions. Journal of Tribology*, Vol. 79, No. 3, 1957, pp. 607–615.

[16] Dombrowski, N., and Hooper, P. C., "A Study of the Sprays Formed by Impinging Jets in Laminar and Turbulent Flow," *Journal of Fluid Mechanics*, Vol. 18, No. 3, 1964, pp. 392–400. doi:10.1017/S0022112064000295

[17] Ryan, H. M., Anderson, W. E., Pal, S., and Santoro, R. J., "Atomization Characteristics of Impinging Liquid Jets," *Journal of Propulsion and Power*, Vol. 11, No. 1, 1995, pp. 135–145.

[18] Anderson, W. E., Ryan, H. M., and Santoro, R. J., "Impact Wave-Based Model of Impinging Jet Atomization," *Atomization and Sprays*, Vol. 16, No. 7, 2006, pp. 791–805. doi:10.1615/AtomizSpr.v16.i7.60

[19] Behroozi, F., "Fluid Viscosity and the Attenuation of Surface Waves: A Derivation Based on Conservation of Energy," *European Journal of Physics*, Vol. 25, No. 1, 2004, pp. 115–122. doi:10.1088/0143-0807/25/1/014

[20] Clark, C. J., and Dombrowski, N., "Aerodynamic Instability and Disintegration of Inviscid Liquid Sheets," *Proceedings of the Royal Society of London A*, Vol. 329, No. 1579, 1972, pp. 467–478. doi:10.1098/rspa.1972.0124

D. Talley
Associate Editor